Journal of Applied Electrochemistry **30**: 711–716, 2000.

Nucleation effects on structural and optical properties of electrodeposited zinc oxide on tin oxide

B. CANAVA and D. LINCOT*
Laboratoire d'Electrochimie et de Chimie Analytique, Unité associée au CNRS (UMR 7575), Ecole Nationale Supérieure de Chimie de Paris, 11 rue Pierre et Marie Curie, 75231 Paris Cedex 05, France
*(*author for correspondence; email: lincot@ext.jussieu.fr)*

Received 14 January 1999; accepted in revised form 19 May 1999

Key words: electrodeposition, nucleation, optical transmission, oxygen reduction, tin oxide, zinc oxide

Abstract

Zinc oxide was electrodeposited from oxygenated aqueous solutions of zinc chloride at 80 °C on tin oxide covered glass substrates. A new activation treatment for the substrate is established. This consists in the initial formation, in the deposition solution, of a thin metallic zinc layer (5–50 nm) converted to ZnO by *in situ* reoxidation. Variable densities of nucleation centers (with values approaching 10^{10} cm^{-2}) are formed by this treatment. This allows control of the formation of a zinc oxide layer ranging from open deposits of isolated crystallites to compact and homogeneous layers. Compact layers have high specular transmission below the band gap value (~3.5 eV), whereas open films exhibit extensive light scattering. The shapes of the current–time curves during deposition are discussed in terms of nucleation and structural effects. A possible influence of the semiconducting properties of the films is pointed out.

1. Introduction

Several studies have been devoted to the electrodeposition of oxide films directly from dissolved precursors, as for instance for cathodic deposition using nitrate ions as the oxygen precursor [1]. It has been discovered only recently that good quality zinc oxide films can be deposited simply using dissolved oxygen as the precursor [2, 3] according to the overall reaction:

$$Zn^{2+} + 0.5\,O_2 + 2\,e^- \rightarrow ZnO \qquad (1)$$

Further studies have shown that the deposition was also possible using nitrate ions [4]. Films of ZnO are used in various applications such as photovoltaics, photoconductive sensors and piezoelectric transducers [5]. In photovoltaics, for instance, they are used as transparent conducting electrodes (TCO) in cells based on copper indium diselenide [6] or amorphous silicon [7] absorbers. Various techniques, mainly from the vapour phase, have been used to prepare ZnO thin films, such as r.f. sputtering [6], metal–organic chemical vapour deposition (MOCVD) [8], molecular beam epitaxy, and atomic layer epitaxy (ALE) [9]. Electrodeposition can now be added to these methods. Owing to the simplicity and low cost of this technique, it may find applications in the future. Recently, we have shown that electrodeposited ZnO films can be used as a TCO in thin film solar cells [10].

An interesting characteristic of the electrodeposition of zinc oxide is the possibility to obtain different morphologies of the deposits. Films with dense or open structures have been described [2]. The open structure consisted of an array of single crystalline ZnO columns. Such structures are potentially very interesting for chemical sensors or solid-state dye-sensitized solar cells where a high surface-to-volume ratio is needed. Another recent application of this type of structure has been presented for electrodeposited calcium carbonate whiskers as cathodes in flat screens [11].

The aim of this work is to better analyse the formation of the open structure of zinc oxide by electrodeposition, with special focus on the role of nucleation effects. Such effects are especially marked when the growth is performed on an inert substrate as tin oxide. In the case of gold substrates, for instance, it has been shown that a strong affinity between gold and zinc leads generally to a compact and covering layer.

We have studied specifically the electrodeposition of zinc oxide on glass substrates covered by a tin oxide layer. The deposition was studied *in situ* by electrochemical techniques as cyclic voltammetry and chronocoulometry. The deposits have been then characterized *ex situ* by scanning electron microscopy (SEM), X-ray diffraction (XRD) and optical transmission. The results show that the properties are critically dependent on the initial nucleation step on the substrate. It is shown that it is possible to control this nucleation step by an *in situ* electrochemical activation of the SnO_2 surface leading to

the formation of a ZnO seed layer with a mean thickness of a few tens of nm.

2. Experimental details

The substrates were glass plates covered by a tin oxide film deposited by spray pyrolysis with a thickness of 0.5 μm and a sheet resistance of 10 $\Omega/\square$. The area of the electrode were about 5 cm^2. Prior to deposition, the substrate surface was degreased using a detergent for 10 s, rinsed in deionised (DI) water (18.2 MΩ cm, Millipore system) and then dipped in a 2 M HCl solution for 10 s at room temperature. Finally, the surface was thoroughly rinsed in DI water. The deposition solution contained 5×10^{-3} M of zinc chloride (Merck, *pro analysi*) and 0.1 M of KCl (Prolabo, normapur analytical reagent) as the supporting electrolyte. The pH at room temperature was 5.8. Oxygen was introduced in solution by bubbling. The concentration between 0 and saturation was fixed by bubbling argon–oxygen mixtures in different ratios. The saturation value is about 10^{-3} M at room temperature and decreases at higher temperature ($\sim 5 \times 10^{-4}$ M at 80 °C) [12].

Electrochemical studies and film depositions were made by using a potentiostat (EG&G model 362) in the three electrode configuration. The reference electrode was a saturated calomel electrode (SCE, $E_0 = 0.244$ V vs SHE, the standard hydrogen electrode). The temperature was controlled within 0.1 °C and agitation of the solution was provided by a magnetic stirrer. The deposition studies were carried out at $T = 80$ °C.

The deposits were studied by scanning electron microscopy (model Jeol JSM T 330A) and optical transmission (double beam u.v.–i.r. Perkin–Elmer Lambda 9 spectrophotometer). The crystalline structure and orientation were determined by X-ray diffraction with a cobalt anticathode ($\lambda = 0.1789$ nm). Resistivity measurements on the detached films (according to a procedure described in [13]) were made by the Van der Pauw method.

3. Results

3.1. *Electrochemical studies*

Figure 1 shows voltammetric curves of SnO_2 in the blank solution (0.1 M, KCl) at $T = 80$ °C without and with oxygen. Without oxygen (curve (a)) there is no electrochemical reaction observed for applied potentials between 0 to −1.2 V. From −1.2 V down to −2 V, we observe an increase in the cathodic current which can be mainly attributed to the reduction of the solvent according to the following reaction:

$$H_2O + e^- \rightarrow OH^- + 0.5\,H_2 \qquad (2)$$

However, we observe that the electrode turns black indicating that there is a parallel reaction which is likely the reduction of tin oxide to metallic tin:

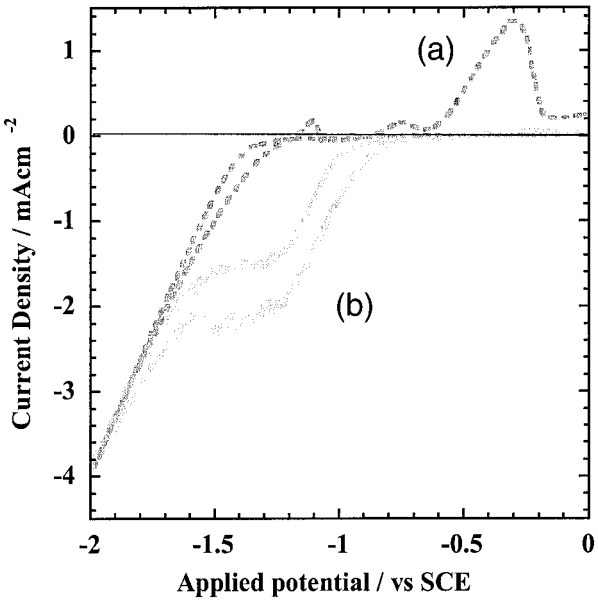

Fig. 1. Voltammograms of SnO_2 substrates in KCl 0.1 M without zinc, $T = 80$ °C, $v = 10$ mV s^{-1}. Curves: (a) Ar saturated, (b) with O_2 at 70% of saturation. Remark: The slope appearing in the current–potential curves is due to the effect of the tin oxide sheet resistance.

$$SnO_{2(s)} + 2\,H_2O + 4\,e^- \rightarrow Sn_{(s)} + 4\,OH^- \qquad (3)$$

In the reverse scan we observe a main anodic peak from −0.64 V which indicates the reoxidation of surface species. This corresponds well to the reoxidation of metallic tin formed in Reaction 3 since the redox potential of the couple $SnO_2/Sn(0)$ is −0.71 V vs SCE at pH 6. In contrast there is a large overpotential for the cathodic decomposition reaction (Reaction 3). Two unidentified minor anodic peaks appear at −1.2 V and −0.8 V.

In the presence of oxygen (curve (b)), the behaviour is modified. From −0.65 V down to −1.3 V, we observe the appearance of a wave which can be assigned to the oxygen reduction according to Reactions 4 and 5 in parallel:

$$O_2 + 2\,H_2O + 4\,e^- \rightarrow 4\,OH^- \qquad (4)$$

$$O_2 + 2\,H_2O + 2\,e^- \rightarrow H_2O_2 + 2\,OH^- \qquad (5)$$

The height of the wave depends on the concentration of oxygen, indicating a diffusion control. Below −1.5 V, the current increases as in curve (a) corresponding to solvent or substrate reduction. In the reverse scan, it is interesting to note that there is no anodic peak of electrodeposited metallic tin. This indicates that oxygen may either prevent the decomposition of tin oxide, or that metallic tin is not stable on the surface in the presence of oxygen (chemical oxidation).

Figure 2 presents the electrochemical behaviour when zinc ions are added into the solution. Without oxygen (curve (a)), there is no electrochemical reaction observed for applied potentials between 0 to −1.15 V. From

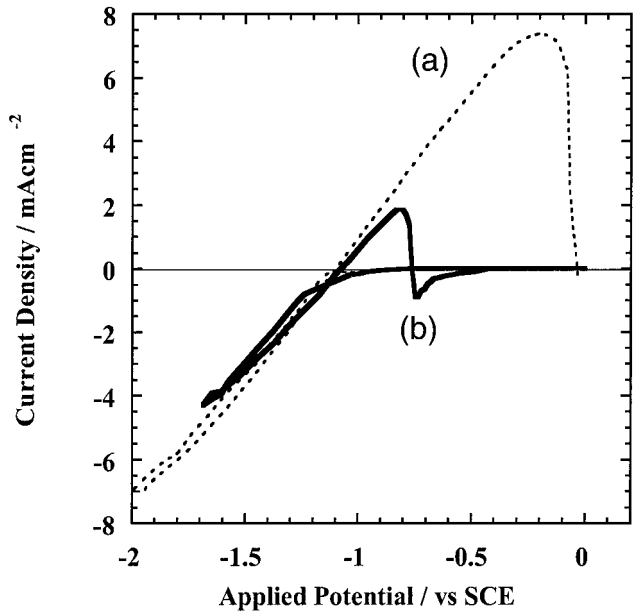

Fig. 2. Voltammograms of SnO_2 substrates in KCl 0.1 M in presence of $ZnCl_2$ (5×10^{-3} M), $T = 80\,^{\circ}C$, $v = 10$ mV s^{-1}. Curves: (a) Ar saturated, (b) with O_2 at 70% of saturation.

-1.15 V and down to -2 V, we observe an increase in the cathodic current. In the reverse scan, from -1.1 V, we observe a anodic peak up to -0.2 V corresponding to the oxidation of electrodeposited metallic zinc on the substrate ($E^{\circ}_{Zn2+/Zn} = -1.07$ V vs SCE at 25 °C). In the presence of oxygen and zinc (curve (b)), we do not observe the expected oxygen reduction. This indicates that the presence of Zn(II) ions hinders the oxygen reduction. This can be attributed to the adsorption of zinc containing species at the surface of tin oxide which blocks the transfer of electrons to oxygen. From -1.15 V down to -1.7 V, the cathodic current increases leading to the deposition of metallic zinc as shown by the presence of an oxidation peak during the reverse scan.

An interesting phenomenon is that immediately after the anodic peak, the current becomes cathodic, appearing as a cathodic spike in Figure 2. This spike is necessarily associated with oxygen reduction as this is the only possible reduction reaction in this potential range. We observe (not shown) that if the potential is now reversed, there is a stationary cathodic current. As a consequence, the predeposition of zinc followed by its reoxidation activates the reduction of oxygen. In fact, the cathodic reaction is no longer reaction 4 but corresponds to the formation of zinc oxide according to Reaction 1 [3].

This zinc reduction/oxidation cycle, leading to the formation of a prelayer of ZnO [3], can be considered as a surface activation treatment. Previously the activation was only obtained after a long cathodic polarization of the tin oxide substrate in presence of oxygen but without zinc [2]. The present treatment is much more simple.

To control the nucleation characteristics we can modify the amount of predeposited zinc by varying the quantity of electricity passed during the cathodic reaction. Figure 3 shows the influence of cathodic activation on zinc oxidation for different values of the charge obtained under galvanostatic conditions. From the area under the reoxidation peak it is possible to calculate the real quantity of deposited zinc. Table 1 shows the values and the calculated equivalent thickness of the layer (with $d = 7.04$ g cm^{-3}, if we assume a bulk density volume). It appears that the faradic efficiency tends to one when the cathodic charge increases allowing control of the equivalent thickness in the nm range. However, the value tends to decrease for lower coverages, about 0.5 for an equivalent thickness of 7 nm. This effect is probably due to solvent reduction evidenced on bare tin oxide (Figure 1). It is also possible that part of the metallic zinc is directly oxidized by dissolved oxygen, this effect being more sensitive at low thicknesses.

After surface activation, cathodic deposition of zinc oxide via Reaction 1 can be carried out under potentiostatic conditions. We observed that the variation of the deposition current as a function of time was greatly dependent on the characteristics of the pretreatment.

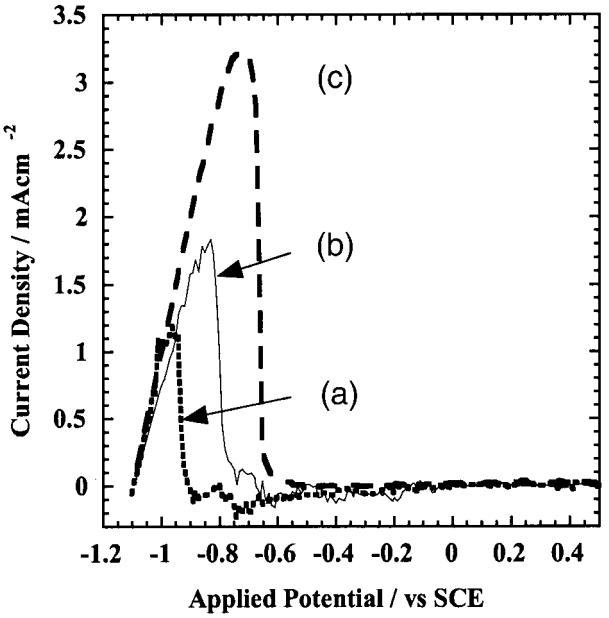

Fig. 3. Anodic oxidation of electrodeposited zinc as a function of the cathodic charge passed during the activation treatment (15 s at different current densities), (a) 12.5, (b) 21 and (c) 31 mC cm^{-2}. Conditions: $[Zn^{2+}] = 5 \times 10^{-3}$ M, KCl 0.1 M, 70% $[O_2]$, $T = 80\,^{\circ}C$, $v = 10$ mV s^{-1}.

Table 1. Quantity of electricity involved in the activation treatments presented in Figure 3. Equivalent thickness assuming 100% faradic efficiency

Cathodic Charge /mC cm^{-2}	Anodic Charge /mC cm^{-2}	Equivalent thickness/nm
21	12	7
37.5	37.2	12.5
93	93	31

Figure 4 shows current vs time curves obtained at a deposition potential of −0.9 V for different cathodic charges: curve (a) is obtained without any cathodic treatment and curves (b) to (d) correspond, respectively, to 4.4, 21.4 and 71.8 mC cm^{-2}. Without activation, the current is initially low and increases progressively with time, decreasing after the peak towards a stationary value. The peak position is at about 500 s. After a very small activation, the shape is the same but the peak position is markedly shifted towards shorter time (75 s). For longer activations, the current is maximum at $t \approx 0$ and directly decreases towards a stationary value. After activation there is an initial anodic transient current (Figure 4(d)) which corresponds to the oxidation of the zinc prelayer. While the trend in peak position with the pretreatment is clear, we observe that the differences in the plateau values do not show clear correlations. Possible reasons can be uncontrolled differences in the hydrodynamic regime, uncertainties in substrate areas or differences in the properties of the films. The differences in the plateau current densities seem to be too large to be only explained by the two first reasons. Differences in conductivity or semiconducting properties of the films is the most plausible explanation.

3.2. *Properties of the films*

3.2.1. *Structural properties*

Figure 5 shows the influence of surface activation on the structure of ZnO deposits as observed by SEM. All the depositions are carried out at −0.9 V during 20 mn. Figure 5(a) corresponds to a deposition without activation, in (b) it is of 15 mC cm^{-2} (1 mA cm^{-2} for 15 s) and in (c) 42 mC cm^{-2} (2.85 mA cm^{-2} for 15 s). For the nonactivated substrate, the deposit has an open structure composed of separate columnar grains with a well-defined cross hexagonal section. The density of grains is about 6×10^8 cm^{-2} as determined by analysis of the micrographs. We note that the size dispersion is low with a mean value of 0.35 μm for the cross section. The orientation of the grains (*c* axis) varies from one grain to the other. The effect of activation is to increase markedly the grain density which passes to 2.5×10^9 cm^{-2} in (b), to 7.7×10^9 cm^{-2} in (c). As shown in Figure 6, the variation seems to be linear. The cross section size concomitantly decreases to 0.2 μm and 0.1 μm, respectively. The increase in grain density favours coalescence between individual grains during lateral growth and explains an increase of the compact-

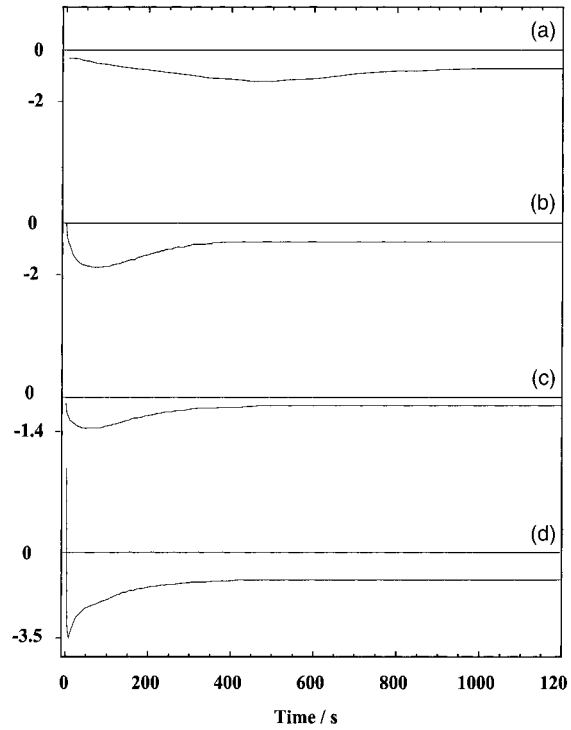

Fig. 4. Current density–time curves for ZnO deposition at −0.9 V vs SCE after different activation treatments: (a) without activation, (b) 4.4 mC cm^{-2} (0.29 mA cm^{-2}, 15 s), (C) 21.4 mC cm^{-2} (1.42 mA cm^{-2}, 15 s) and (d) 71.8 mC cm^{-2} (4.79 mA cm^{-2}, 15 s). Same conditions in solution as Figure 3.

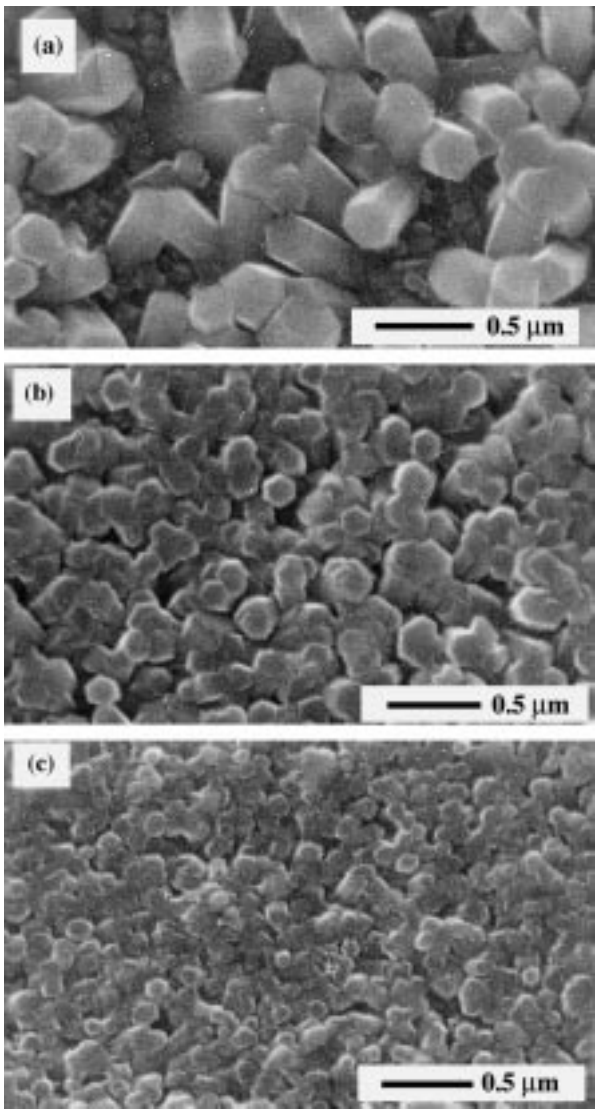

Fig. 5. SEM micrographs of electrodeposited zinc oxide as a function of the activation treatment. Same deposition conditions as in Figure 4. Duration: 20 min. (a) No activation, (b) 15 mC cm^{-2} (1 mA cm^{-2}, 1 s), (c) 42 mC cm^{-2} (2.85 mA cm^{-2}, 15 s).

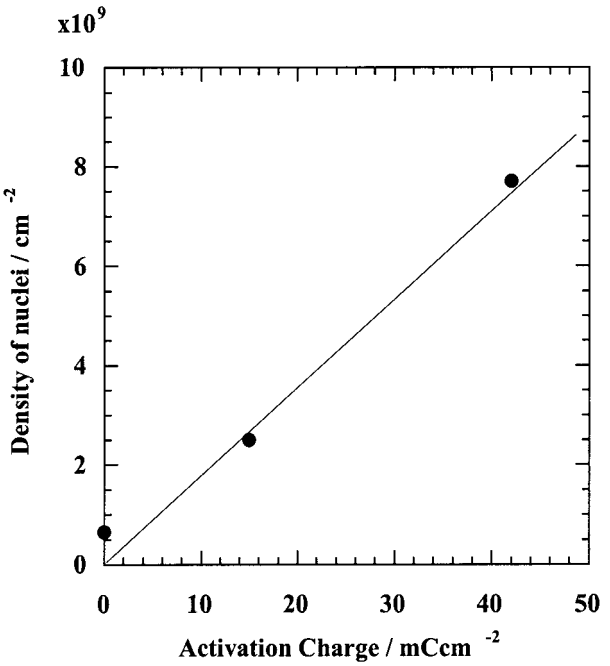

Fig. 6. Density of nucleation centres as a function of the activation treatment, corresponding to the experiments of Figure 5.

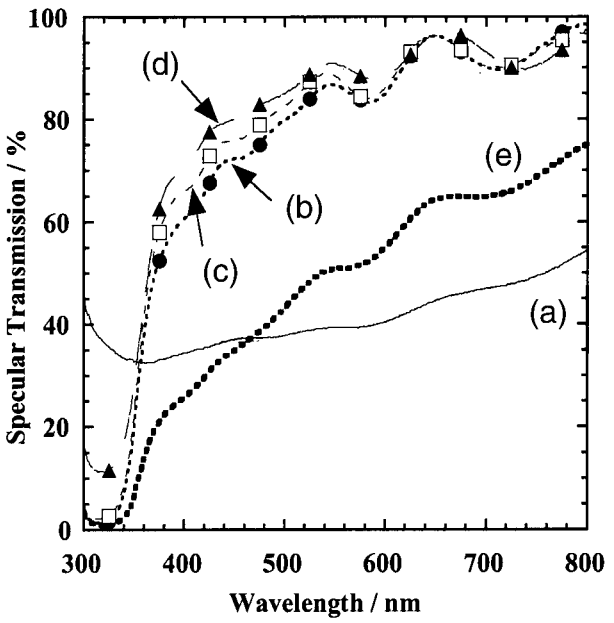

Fig. 7. Influence of the activation treatment on specular optical transmission of electrodeposited ZnO. Deposition conditions are the same as in Figure 3. (a) No activation, (b) 4.5 mC cm^{-2} (0.3 mA cm^{-2}, 15 s), (c) 21 mC cm^{-2} (1.45 mA cm^{-2}, 15 s), (d) 43 mC cm^{-2} (2.85 mA cm^{-2}, 15 s), (e) 86 mC cm^{-2} (5.7 mA cm^{-2}, 15 s).

ness of the deposit with the activation treatment. Coalescence between grains is clearly seen in Figure 5(b). It appears that the grains merge intimately together which is important for applications where nonporous films are needed. The activation also seems to increase the preferential orientation with the *c* axis of ZnO perpendicular to the surface.

3.2.2. *Optical properties*

Figure 7 shows the specular optical transmission of ZnO films as a function of the activation treatment. The activation is carried out galvanostatically during 15 s but similar results have been obtained in the potentiostatic mode.

The most important effect appears when comparing activated and unactivated substrates. For activated substrate, we observe the behaviour expected for an homogeneous semiconducting film with a steep transmission onset for wavelengths higher than the band gap value (0.35 μm for ZnO). The transmission is level is high indicating a high transparency of the films. It appears that there is an optimal activation charge, with best results for about 40 mC cm^{-2}. For higher values there is a decrease in the transmission properties (note that the transmission onset at 0.35 μm for 86 mC cm^{-2} is still sharp). This may be due to a too thick initial seed layer of zinc which can perturb light transmission, by incomplete oxidation or by an increased light scattering effect for wavelengths below the band edge value. The second explanation is more likely since a metallic layer should leads to uniform attenuation as a function of wavelength. For the unactivated substrate a completely different behaviour takes place. There is no more transmission onset and the transmission is much lower in the visible range (40% instead of 80%). Such a behavior is directly related to the structure of the film. As shown by SEM views and XRD in these conditions the film is not compact and composed of individual grains with a more or less random orientation, whereas for an activated substrate it is compact and uniform. This markedly increases light scattering and consequently decreases the specular part of the transmitted light in agreement with the results. This effect is also visible to the eyes, the films on nonactivated substrates are milkywhite instead of transparent as for the activated ones. We have checked that when measuring the total transmitted light with an integrating sphere, the high transmission level is recovered in the visible range, together with the presence of the transmission onset characteristic of ZnO. The last point to explain is the high transmission level for wavelengths shorter than the gap value. This is simply due to the non-compact nature of the films, as parts of the substrate area are not covered with ZnO and they transmit light without u.v. absorption (see Figure 4(a)).

3.2.3. *Electrical properties*

Electrical properties of the films have been addressed by resistivity measurements in the van der Pauw configuration. As the substrate is conductive, the ZnO layer had to be removed prior to measurements. This has been done with thick ZnO layers (up to 10 μm) using the epoxy resin method [13]. Resistivity measurements give a value of $\rho \approx 0.1\,\Omega$ cm, indicating that the films are conducting. The origin of this doping can be attributed to nonstoichiometry of the films (oxygen vacancies or

zinc interstitial) or to extrinsic doping with the substitution of oxygen atoms by chlorine atoms.

4. Discussion

An important aspect concerns the relations between the deposition current and the properties of the deposits. We have shown that the deposition current vs time reaches a peak followed by a stationary value. The initial increase in current is characteristic of the effect of nucleation processes in electrocrystallization of metals. Due to the formation and the growth of nuclei, the deposition current increases progressively from zero with a rate which increases with the density of nucleation centres [14]. This is in clear agreement with SEM results showing that the activation treatment provides additional seeds for the growth of ZnO as compared to the bare substrate. As the surface tends to be completely active, the deposition starts without delay. Similar behaviour has been found previously on gold substrates without activation [3]. The fact that the grains have a small dispersion in size further indicates that the nucleation is more likely instantaneous than progressive.

The presence of a peak is a striking feature of ZnO deposition. For metal deposition, peaks are classically attributed to the effect of diffusion as a rate limiting step. Peaks in i/t profiles are not only observed for metal but for semiconductor deposition as CdTe [15]. However the time scale involved should be of the order of a few seconds according to the dynamics of equilibration processes in the diffusion layer near the surface [14]. In the present case, the peak position is situated at much longer times (500 s), especially for non-activated substrates. This indicates that factors other than diffusion from solution are probably involved in the decrease of the current. Such factors can be kinetic limitations due to electron transport in the solid or to electron transfer at the interface. In the extreme case of an insulating material, it is clear that the current should decrease to zero. In the present case, the decrease with a non-zero stationary current value can be explained by the fact that ZnO is conducting. However as a n-type semiconductor, the surface concentration of electrons available for charge transfer is much lower than for a metallic electrode. This favors kinetic limitations as compared to a metallic electrode. At the initial stages of growth, higher currents are explained by the low thickness of the deposit which allows surface concentrations of electrons higher than the stationary value on a thick electrode (equivalent to a semiinfinite electrode). This points out the importance of considering the effect of semiconducting properties of the deposit in further studies.

5. Conclusions

We have studied a new activation treatment for the growth of zinc oxide films on tin oxide substrates, with special focus on electrochemical aspects. The activation consists of an *in situ* formation of a ZnO seed layer. High densities of nucleation centers (with values approaching 10^{10} cm^{-2}) are associated with this treatment. This allows control of the formation of the subsequent zinc oxide layer from open deposits made of individual crystallites to compact and homogeneous layers. Compact layers have high specular transmission below the band gap value ($\sim$3.5 eV) whereas open films are highly scattering. These films may be useful for specific applications as transparent n-type windows in solar cells or for sensors devices where high developed surface areas are needed.

References

1. J.A. Switzer, *Am. Ceram. Bull.* **66** (1987) 1521.
2. S. Peulon and D. Lincot, *Adv. Mater.* **8** (1996) 166.
3. S. Peulon and D. Lincot, *J. Electrochem. Soc.* **145** (1998) 864.
4. M. Isaki and T. Omi, *Appl. Phys. Lett.* **68** (1996) 2439.
5. M.J. Vellekop, A. Venema, C. Visser and P.M. Sarro, *Am. Ceram. Soc. Bull.* **69** (1990) 1503.
6. L. Stolt, J. Hedström, M.Rückh, J. Kessler, K.O. Velthaus and H.W. Schock, *Appl. Phys. Lett.* **62** (1993) 597.
7. T. Ikeda, J. Sato, Y. Hayashi, Y. Wakayama, K. Adachi and H. Nishimura, *Sol. Energy Mater. Sol. Cells* **34** (1994) 379.
8. W.W. Wenas, A. Yamada, M. Konagai and K. Takahashi, *J. Appl. Phys.* **33** (1994) 283.
9. B. Sang and M. Konagai, *J. Appl. Phys.* **35** (1996) 602.
10. D. Lincot, B. Canava, S. Quenet, S. Peulon and H.W. Schock, Proceedings of the 14th European Photovoltaic Solar Energy Conference, H.S. Stephens & Associates, (1998), p. 2168.
11. D. Zhou, E.V. Anoishhkina, V.H. Desai, K.J. Casey, *Electrochem. Solid State Lett.* **1** (1998) 111.
12. K. Kinoshita, *in* '*Electrochemical Oxygen Technology*' (J. Wiley & Sons, New York, Electrochemical Society, 1992).
13. J.A. von Windheim, H. Wynands and M. Cocivera, *J. Electrochem. Soc.* **138** (1991) 11.
14. R. Greef, R. Peat, L. M. Peter, D. Pletcher and J. Robinson, *in* 'Instrumental Methods in Electrochemistry' (Ellis Horwood, 1985), p. 304.
15. E. Mori and K. Rajeshwar, *J. Electroanal. Chem.* **258** (1989) 415–29.